Shear Degradation of Water-Soluble Polymers. I. Degradation of Polyacrylamide in a High-Shear Couette Viscometer

A. H. ABDEL-ALIM and A. E. HAMIELEC, *Department of Chemical Engineering, McMaster University, Hamilton, Canada*

Synopsis

This manuscript reports an experimental investigation of the mechanical degradation of polyacrylamide in aqueous solution using a high-shear couette viscometer. Equilibrium molecular weight distributions (MWD) at various shear stresses were measured by gel permeation chromatography. Degradation data indicate that the MWD becomes narrower at higher shear stresses, in general agreement with Bueche's midpoint break theory. An empirical correlation of the critical molecular weight and degrading shear stress is presented. It has the form

$$M_c = \frac{3.59 \times 10^8}{\tau^{0.41}}$$

where M_c is the critical molecular weight and τ is the degrading shear stress in dynes/cm².

INTRODUCTION

Mechanical degradation of high polymers has become increasingly important as new applications for supermolecular weight polymers develop. Among these applications is the use of water-soluble polymers in drag reduction and as flocculating agents in waste water treatment. In these applications, polymer molecules are exposed to shear action which can cause chain degradation. Larger molecules contribute more in the aforementioned applications; it is therefore important to study the shear degradation of these molecules to establish limits for their use.

Polyacrylamide is well known for its use in drag reduction, as a thickening agent, and as a flocculant in water treatment. Only very recently has shear degradation of this polymer received attention. Wade and Kumar[1] degraded dilute aqueous solutions of polyacrylamide by forcing the solutions through a fine capillary. They used electron microscopy to follow the molecular weight distribution variation with number of passes through the capillary. In capillary flow, the shear field is not uniform and only a small fraction of the polymer experiences the wall shear stress per pass. The polymer experiences a distribution of shear stress across the radius of the capillary and makes interpretation of degradation measurements very difficult. The same holds true with the use of an ultrasonic generator.
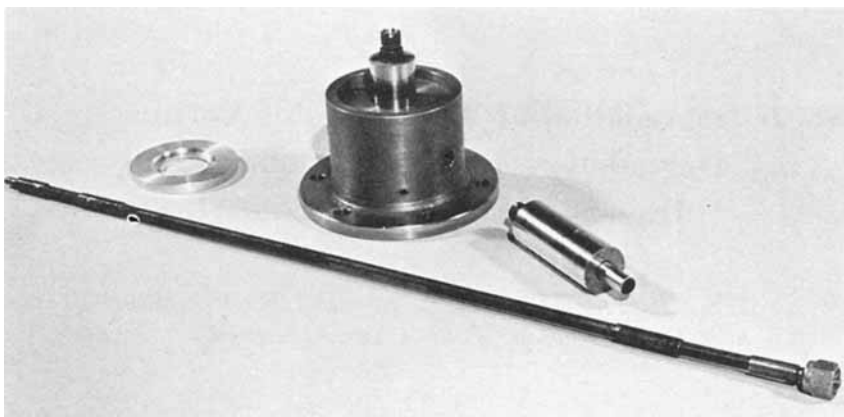
Fig. 1. Concentric cylinder assembly and semiflexible shaft.

In the present work, we used a high-shear couette flow viscometer with a very narrow gap. This offers many advantages, e.g., a well-defined and uniform shear field, high rates of shear up to about 10^6 sec^{-1}, no corrections for end effects, and very small amounts of the polymer needed. This viscometer enables one to vary the shear rate simply by changing the rpm of the inner cylinder, and so it offers the opportunity to perform a series of equilibrium degradation experiments at different shear rates. Equilibrium degradation is achieved in less than a minute.

Porter, Cantow, and Johnson[2-5] used a similar high-shear viscometer to study shear degradation of polyisobutene. They used gel permeation chromatography (GPC) to measure the molecular weight distribution at different stages of degradation. GPC was also used in this work, and this enabled us to follow the molecular weight distribution change with shear stress.

EXPERIMENTAL

The High-Shear Viscometer

A concentric-cylinder rotational viscometer with a very narrow gap between the cylinders was used (0.001 ± 0.00001 in.). The viscometer is equipped with a thermostating system to allow measurements at different temperatures. The instrument is very similar to those used by Barber,[6] Reches,[7] and Porter.[2-5] In a previous publication[8] we gave a detailed description of the viscometer including all the modifications that were found necessary. Figure 1 shows a photograph of the concentric cylinder assembly and the semiflexible drive shaft that we used to eliminate the eccentricity problem.[8]

GPC Measurements

A Waters ALC/GPC 301 was used, under the following conditions: sample volume injected, 2 ml; solvent, distilled water (25°C); polymer con-

centration, 0.01 wt-%; max. sensitivity; flow rate, 3 ml/min; and five columns in series of the following specifications: CPG-10, 2500 Å; CPG-10, 2000 Å; Porasil DX, 400–800 Å; Porasil CX, 200–400 Å; CPG-10, 125–240–370 Å. The columns were calibrated using broad standards of polyacrylamide of known molecular weight distribution employing a technique that was recently developed to calibrate GPC for water-soluble polymers.[9]

Materials and Experimental Conditions

Polyhall 402, a nonionic polyacrylamide (supplied by Stein-Hall Ltd.) was used. The polymer is water soluble and solutions in water are very viscous even in dilute concentrations. This puts an upper limit on the concentrations to be used, in fact, a solution of concentration more than 2% by weight is essentially a solid gel. Two concentrations were investigated in this work, 0.2% and 0.7% by weight. Temperatures employed were 25°C and 40°C.

Procedure

The polymer solution was injected into the viscometer using a glass syringe fitted with a filter. The inner cylinder was then removed and washed carefully with a known amount of distilled water, and the concentration of the wash liquid was adjusted to about 0.01 wt-% prior to GPC analysis. This first GPC injection is considered the undegraded polymer. In this way we eliminate the error due to possible degradation caused by the injection process. The viscometer is then cleaned and the gap is refilled with polymer solution. The shear rate is then increased by rotating the inner cylinder at increasing rpm in steps. At each shear rate equilibrium conditions were established when the recorded torque leveled off to a steady-state value. This never required more than 1 min of time. After equilibrium was reached, the rpm was decreased again to the previous value. Degradation is indicated by a permanent loss in viscosity; a reversible path indicates no degradation. When degradation was noticed at certain shear conditions, the instrument was stopped, the inner cylinder taken out, washed as described above, and a GPC injection was made. Following this, the instrument was cleaned and refilled. Shear rate was increased to a higher level this time and the process repeated.

RESULTS

Figure 2 shows the effect of shear rate on the viscosity of the 0.7 wt-% solution at 25°C. The viscosity was recorded at a shear rate of 2.6×10^3 sec^{-1}. The shear rate was increased to 5.2×10^3 sec^{-1}. On going back to 2.6×10^3 sec^{-1}, a lower viscosity was recorded indicating shear degradation. The solid lines with arrows at both ends indicate reversible paths, while dashed lines with arrows at one end indicate irreversible paths or degradation paths.

TABLE I
Summary of Experimental Data

| Run	Concentration, wt-%	Temp., °C	Shear rate, $\times 10^{-4}$ sec^{-1}	Equilibrium viscosity, poise	Shear stress, $\times 10^{-4}$ dynes/cm²	Critical molecular wt. $M_c \times 10^{-6}$	$M_n \times 10^{-6}$	$M_v \times 10^{-6}$	M_w/M_n	Symbols
13	0.2	25	4.20	0.34	1.43	6.79	2.38	5.76	2.42	▲
14	0.2	25	7.32	0.25	1.90	6.50	2.35	5.36	2.28	
15	0.2	25	10.4	0.21	2.18	5.82	2.21	4.79	2.17	
16	0.2	25	11.5	0.20	2.30	5.61	2.23	4.75	2.13	
20	0.7	40	2.51	0.66	1.65	6.50	2.34	5.41	2.31	●
21	0.7	40	4.20	0.51	2.14	5.91	2.24	5.08	2.27	
22	0.7	40	7.32	0.38	2.78	5.50	2.15	4.54	2.11	
23	0.7	40	10.4	0.31	3.22	4.94	2.05	4.16	2.03	
24	0.7	40	11.5	0.30	3.45	4.92	2.02	3.98	1.97	
26	0.7	25	0.52	2.84	1.48	6.80	2.43	5.83	2.40	○
27	0.7	25	1.56	1.65	2.57	5.55	2.14	4.49	2.10	
28	0.7	25	2.51	1.29	3.24	5.00	2.08	4.16	2.00	
29	0.7	25	4.20	0.95	3.99	4.50	1.93	3.67	1.90	
30	0.7	25	7.32	0.67	4.90	4.25	1.91	3.38	1.77	
31	0.7	25	10.4	0.53	5.51	3.95	1.82	3.19	1.75	
32	0.7	25	11.5	0.50	5.75	3.90	1.84	3.13	1.70	
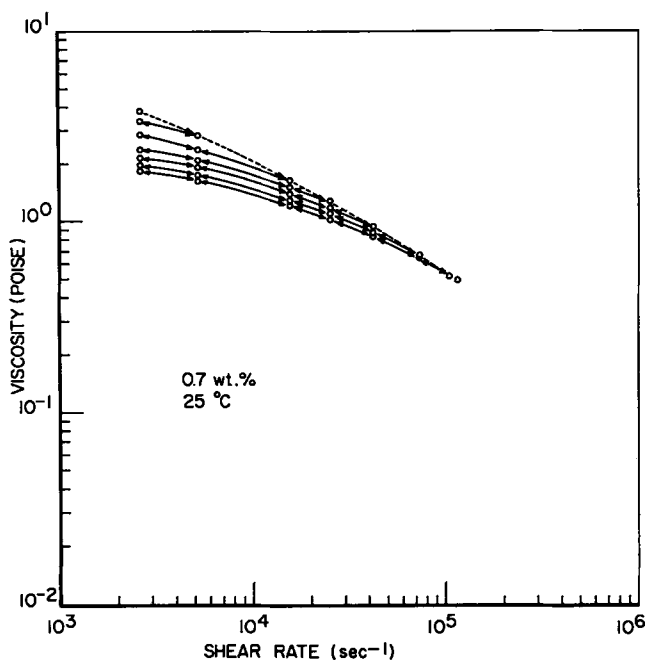
Fig. 2. Effect of shearing at 25°C on the 0.7 wt-% solution.

Figure 3 shows the results for the 0.2 wt-% solution at 25°C. Figures 4 and 5 are for the 0.2% and 0.7% solutions, respectively, at 40°C. It is interesting to note that in Figure 4 we do not get any degradation at all in the range of shear rates used.

Figure 6 shows the molecular weight distributions (differential and cumulative) for the undegraded polymer and for two of the degraded polymers corresponding to runs 28 and 32 in Table I. Table I summarizes all the degradation results. The sixth column in the table is the degrading shear stress obtained directly from the measured torque. The viscosity in the fifth column is obtained by dividing the shear stress by the shear rate. The last column in the table is the critical molecular weight (M_c) which is the maximum molecular weight present at the specified shearing conditions, obtained from the GPC analysis.

In runs 31 and 32 (highest shear stresses), GPC analyses of degradation products indicated the formation of a low molecular weight peak made up of molecules of chain lengths ranging between 5 and 20 monomer units. In a similar study of shear degradation of polyisobutene, Porter et al.[3] noticed such a low molecular weight peak in their degradation products. Figure 7 shows the molecular weight distribution for degraded polymer run 32. The area of the low molecular weight peak is about one third (33%) of the larger one. Comparison of the distribution of run 32 with the less severe runs indicates that the low molecular weight products comes from molecules covering essentially the whole range of the big peak. In other words, the low molecular weight products do not seem to come from a certain molecular size of the degraded polymer.
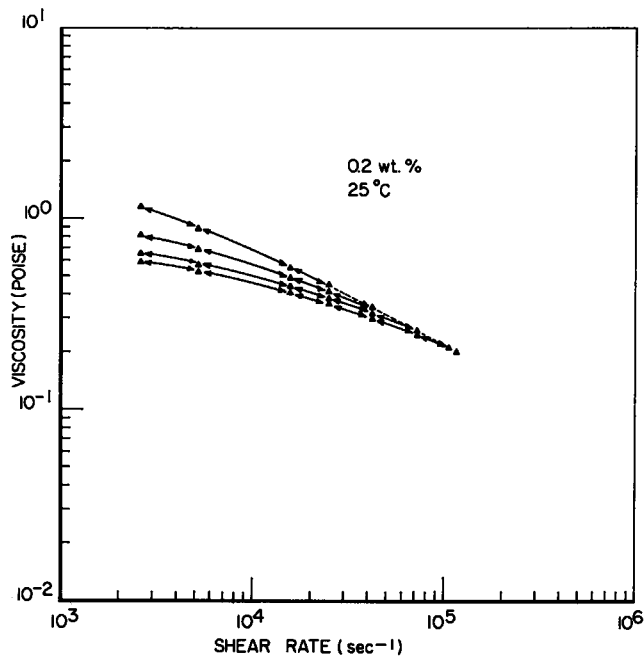
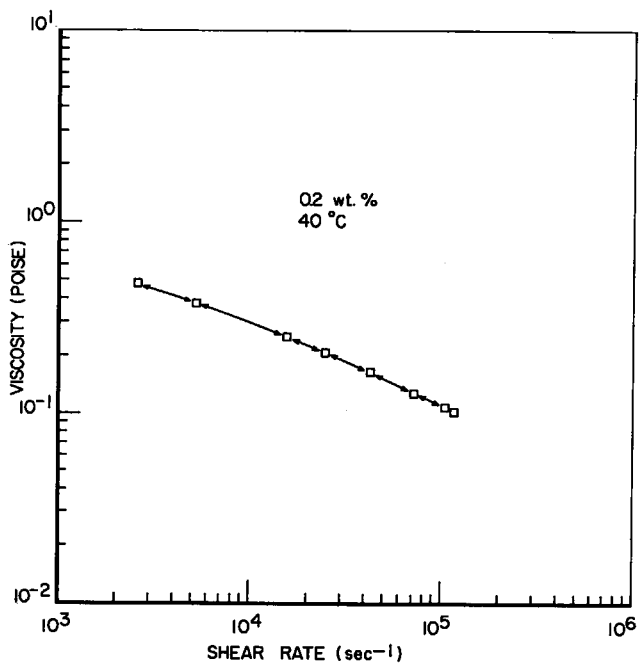Fig. 3. Effect of shearing at 25°C on the 0.2 wt-% solution.

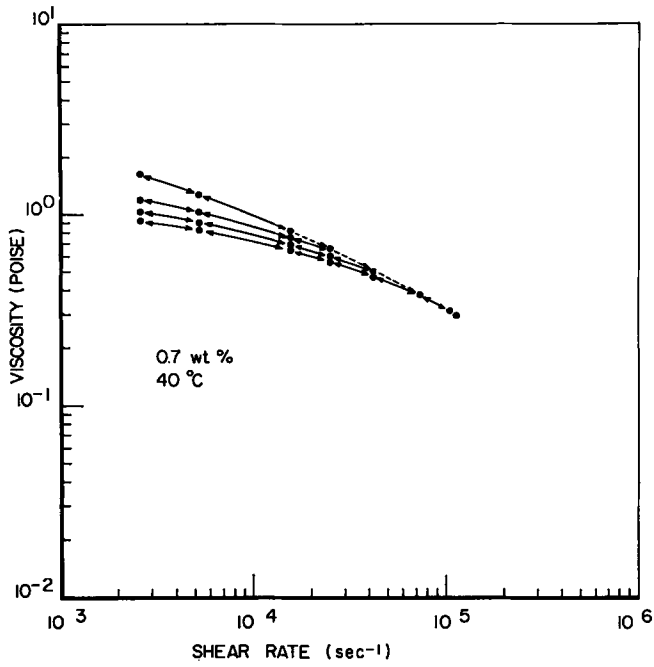Fig. 4. Effect of shearing at 40°C on the 0.2 wt-% solution.

Fig. 5. Effect of shearing at 40°C on the 0.7 wt-% solution.
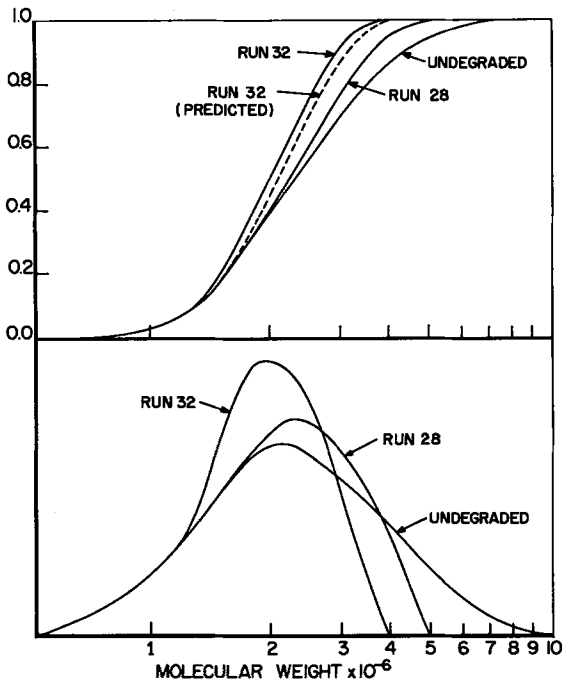

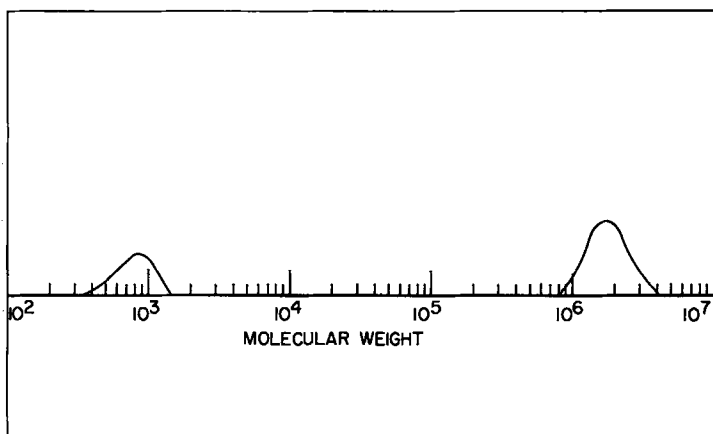Fig. 6. Effect of shearing on the molecular weight distribution.
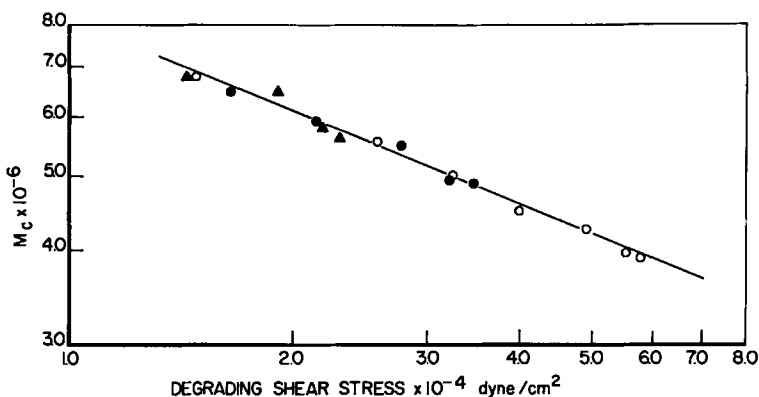
Fig. 7. Bimodal degradation product of run 32.

Fig. 8. Logarithmic plot of critical molecular weight vs. degrading shear stress.

Figure 8 is a logarithmic plot of the critical molecular weight, as defined above and obtained from the GPC trace, versus the degrading shear stress. The relation is reasonably linear on a logarithmic plot.

DISCUSSION

As mentioned above, it was noticed that Figure 4 does not show any degradation for the 0.2 wt-% solution at 40°C. The highest shear stress obtained under these conditions was 1.17×10^4 dynes/cm², corresponding to shear rate of 1.15×10^5 sec^{-1}. From Table I we see that the minimum shear stress noticed to cause polymer degradation is 1.43×10^4 dynes/cm² (the first line in Table I). From this it becomes evident that shear stress, not shear rate, is the controlling factor in shear degradation. Some degradation effects were obtained at equal shear stresses regardless of the value of the shear rate in the range studied. The effect of temperature and concentration on degradation is then simply a result of their effect on viscosity. At a constant shear rate, a decrease in temperature or increase in concentration leads to higher viscosity and higher shear stress and ac-

cordingly more degradation. GPC analyses show that the low end of the molecular weight distribution does not change under degradation. The high end, however, shows a continuous decrease in molecular weight with increasing the shear stress. This results in a narrowing of the distribution. These results seem to support Bueche's theory[10] of mechanical degradation. According to this theory, chain breaking does not take place at random along the chain but occurs predominantly in the central portion of the chain where the extending forces are maximum. The theory assumes the presence of molecular entanglements to be necessary for shear degradation. In the case of polyacrylamide, entanglements should persist even at low concentrations due to the polar nature of the polymer. The theory states that for a polydispersed polymer, all the chains with molecular weight higher than a certain critical size M_c will be broken down into low molecular weight material. All the original polymer having molecular weight $M_1 >$ M_c will appear in the final product as molecular weight $M_1/2^n$, where n is the smallest integer to make $M_1/2^n < M_c$. The value of M_c depends on the shear rate and the viscosity. The higher the viscosity and shear rate, the lower will be M_c.

M_c is easily measured at any degrading shear stress by injecting the degraded polymer in GPC; M_c will be the highest molecular weight in the distribution. For degraded polymer, GPC indicates a well-defined critical molecular weight. This is shown in Figure 6 for runs 28 and 32. The undegraded polymer has a high molecular weight end which is less well defined. Values of degrading shear stresses and the corresponding M_c are given in Table I. A logarithmic plot of these data is shown in Figure 8. The least-squares linear fit yields the following relationship:

$$M_c = \frac{3.59 \times 10^8}{\tau^{0.41}}$$

where τ is the degrading shear stress in dynes/cm². Using the above correlation, we can see that low shear stresses would degrade only very high molecular weight material. For example:

τ, dynes/cm²	M_c
10	13.98×10^7
100	5.44×10^7
1000	2.11×10^7

The above correlation should find use for the estimation of the stability to mechanical degradation of a polymer in applications involving shear field.

The dashed line in Figure 6 is a theoretical prediction of the cumulative molecular weight distribution for run 32. It was obtained from the cumulative distribution of run 28 by straightforward application of the idealized theory of midpoint break. The original undegraded polymer has a disperse high molecular weight tail. M_c for run 32 is 3.9×10^6; according to the theory, all molecules ranging between 3.9×10^6 and 5.0×10^6 (M_c for run 28) should break in the middle. In this case, $n = 1$ since 5.0/2 is less than 3.9. Since molecules of molecular weight 5.0×10^6 would yield molecules of molecular weight 2.5×10^6 on breaking, the fraction of the

polymer of molecular weight between 2.5 and 3.9×10^6 should not change, and graphically this means that the fraction of the original distribution between 2.5 and 3.9 is projected unchanged onto the new distribution. The fraction of the new distribution having molecular weights in the range 1.95 $\times 10^6$ to 2.5×10^6 is simply that in the original polymer plus the fraction of the original polymer between 3.9×10^6 and 5.0×10^6. In this way the predicted distribution can be constructed. The agreement between theory and experiments is not very good. In fact, some of the molecules will break at different distances from the center of the chain, and this should lead to a distribution broader than the midpoint theory prediction. Such a distribution would agree better with experimental observations.

The low molecular weight material observed in runs 31 and 32 is further evidence that Bueche's theory is not valid, particularly at higher shear rates. A possible explanation for the formation of very short chains, however, could be that at these elevated shear stresses the polymer chain breaks before it has time to extend appreciably. At lower shear stresses, degradation does not occur until the polymer chain has extended its conformation appreciably. In other words, chain degradation occurs before equilibrium conformation is obtained and during the approach to conformational equilibrium a polymer chain can experience many breaks.

In a recent study of degradation of polystyrene using ultrasonics, Glynn et al.[11,12] also found that their experimental MWD's were in disagreement with calculated MWD's based on a model which allows breakage at the midpoint of the polymer chain only. A Gaussian probability distribution for the location of rupture sites along the chain and centered around the midpoint gave good agreement with experiment for up to 15 breaks per original polymer molecule. For our lower shear rate experiments, this approach appears promising. However, the results at high shear rates where a second MWD of very low molecular weight polymer is formed as a degradation product are radically different and would require a distribution with a mean near the chain end.

References

1. J. H. T. Wade, and P. Kumar, *J. Hydronautics*, **6**, (No. 1), 40 (1972).
2. R. Porter, M. Cantow, and J. Johnson, *Polymer*, **8**, 87 (1967).
3. R. Porter, M. Cantow, and J. Johnson, *J. Polym. Sci. C*, **16**, 1 (1967).
4. M. Cantow, R. Porter, and J. Johnson, *J. Polym. Sci. C*, **16**, 13 (1967).
5. R. Porter and J. Johnson, *J. Appl. Phys.*, **35**, 3149 (1964).
6. E. Barber, J. Muenger, and F. Villforth, *Ann. Chem.*, **27**, 3 (1955).
7. E. Reches, Ph.D. Thesis, University of Cincinnati, 1967.
8. A. H. Abdel-Alim, S. T. Balke, and A. E. Hamielec, *J. Appl. Polym. Sci.*, **17**, 1431 (1973).
9. A. H. Abdel-Alim and A. E. Hamielec, *J. Appl. Polym. Sci.*, in press.
10. F. Bueche, *J. Appl. Polym. Sci.*, **4** (10), 101 (1960).
11. P. A. R. Glynn, B. M. E. Van der Hoff, P. M. and Reilly, *J. Macromol. Sci.—Chem.*, **A6** (8), 1653 (1972).
12. P. A. R. Glynn and B. M. E. Van der Hoff, *J. Macromol. Sci.—Chem.*, in press.